The Laryngoscope
Lippincott Williams & Wilkins, Inc.
© 2005 The American Laryngological,
Rhinological and Otological Society, Inc.

A Quantitative Study of the Medial Surface Dynamics of an In Vivo Canine Vocal Fold during Phonation

Michael Doellinger, PhD; David A. Berry, PhD; Gerald S. Berke, MD

Objectives/Hypothesis: **The purpose of this study was to measure the medial surface dynamics of a canine vocal fold during phonation. In particular, displacements, velocities, accelerations, and relative phase velocities of vocal fold fleshpoints were reported across the entire medial surface. Although the medial surface dynamics have a profound influence on voice production, such data are rare because of the inaccessibility of the vocal folds.** ***Study Design:*** **Medial surface dynamics were investigated during both normal and fry-like phonation as a function of innervation to the recurrent laryngeal nerve for conditions of constant glottal airflow.** ***Methods:*** **An in vivo canine model was used. The larynx was dissected similar to methods described in previous excised hemilarynx experiments. Phonation was induced with artificial airflow and innervation to the recurrent laryngeal nerve. The recordings were obtained using a high-speed digital imaging system. Three dimensional coordinates were computed for fleshpoints along the entire medial surface. The trajectories of the fleshpoints were preprocessed using the method of Empirical Eigenfunctions.** ***Results:*** **Although considerable variability existed within the data, in general, the medial-lateral displacements and vertical displacements of the vocal fold fleshpoints were large compared with anterior-posterior displacements. For both normal and fry-like phonation, the largest displacements and velocities were concentrated in the upper medial portion. During normal phonation, the mucosal wave propagated primarily in a vertical direction. Above a certain threshold of subglottal pressure (or stimulation to the recurrent laryngeal nerve), an abrupt transition from chest-like to fry-like phonation was observed.** ***Conclusions:*** **The study reports unique, quantitative data regarding the medial surface dynamics of an in vivo canine vocal fold during phonation, capturing both chest-like and fry-like vibration patterns. These data quantify a complex set of dynamics. The mathematical modeling of such complexity is still in its infancy and requires quantitative data of this nature for development, validation, and testing.** ***Key Words:*** **Vocal fold vibration, quantitative measurements, medial surface, hemilarynx, high-speed imaging.**

Laryngoscope, **115:1646–1654, 2005**

INTRODUCTION

Quantitative measurement of the medial surface dynamics of the vocal folds is important for understanding how sound is generated within the larynx. However, such data are difficult to obtain because of the inaccessibility of the vocal folds. Because of the small size and inaccessibility of the larynx, the possibilities for imaging vocal fold oscillations are limited. Traditionally, in vivo high-speed recordings have been performed using endoscopic techniques that yield only a superior view of the vocal folds. Because of this orientation, the medial surface of the vocal folds cannot be seen during glottal closure. Indeed, many aspects of mucosal wave propagation are obscured during the glottal cycle, including the phase delay between the lower and upper part of the vocal folds, which is critical for maintaining normal phonation and which may be used to estimate the viscoelastic properties of vocal fold tissues.[1]

Using an in vivo hemilarynx methodology presented earlier,[2] the present study reported the medial surface dynamics of an in vivo canine vocal fold during phonation as a function of innervation to the recurrent laryngeal nerve (RLN), for conditions of constant glottal flow. In particular, displacements, velocities, accelerations, and relative phase velocities of vocal fold fleshpoints were reported across the entire medial surface of the vocal fold. Minimum glottal area was also analyzed. Where possible, results were discussed and compared with previous observations and hypotheses regarding vocal fold vibration.

MATERIALS AND METHODS

Experimental Set-Up

A male mongrel canine (25 kg) was selected for the study. The animal experiment described in this manuscript was permit-

From The Laryngeal Dynamics Laboratory, Division of Head and Neck Surgery, UCLA School of Medicine, Los Angeles, California, U.S.A.

Editor's Note: This Manuscript was accepted for publication June 8, 2005.

Supported by Grant DC003072 from NIH/NIDCD.

Send Correspondence to Michael Doellinger, The Laryngeal Dynamics Laboratory, Division of Head and Neck Surgery, UCLA School of Medicine, 31-24 Rehab Center, 1000 Veteran Avenue, Los Angeles, CA 90095-1794. E-mail: michael.doellinger@gmx.net

DOI: 10.1097/01.mlg.0000175068.25914.61

Copyright © The American Laryngological, Rhinological and Otological Society, Inc. Unauthorized reproduction of this article is prohibited

ted by the Chancellor's Animal Research Committee of the Office for Protection of Research Subjects at the University of California, Los Angeles (approval no. 2001-122). The canine was premedicated intramuscularly with acepromazine and Buprenex. Over the course of the experiment, halothane ventilation and intravenous pentobarbital was administered to prevent reflexive response to corneal stimulation. After the experiment, the canine was humanely killed with intravenous Eutha-6.

Although the experimental set-up in this study has been discussed in detail elsewhere,[2] a brief description is given as follows.The canine was placed supine on an operating table. A hemilarynx was created through means of a neck dissection and a hemilaryngectomy, which included removal of half of the hyoid bone (Fig. 1). To provide a controlled air supply for phonation, air was insufflated rostrally through a tracheostomy. The air was heated and humidified. The canine was assist-ventilated by way of an endotracheal tube.

So that specific fleshpoints could be tracked during the experiment, small, black, monofilament nylon microsutures were placed on the medial surface of the vocal fold (diameter 0.034 mm). To minimize disturbance of the natural dynamics, the microsutures were positioned to penetrate only the mucosal epithelium. Five columns of microsutures with five microsutures per column were mounted along the medial-superior surface of the vocal fold, where the greatest amplitudes of vibration were expected to occur (Fig. 2). The physical distance between the mounted fleshpoints was 3.10 ± 0.16 mm in the anterior-posterior direction and 2.09 ± 0.24 mm in the vertical direction (Fig. 2).

Next, the trachea was mounted over a stainless steel cylindrical tube. A wedge was mounted within the tube to smoothly channel the airflow beneath the vocal fold. At the top of the tube, a glass plate was mounted (Fig. 1). To eliminate airflow leaks between the vocal fold and the glass plate anteriorly and posteriorly, strips of gauze, coated with vacuum grease, were inserted between them (Fig. 2).

For calibration purposes, a brass cube (5.0^3 mm^3) was glued to the glass plate superior to the vocal fold (Fig. 2). The cube was large enough that one could identify its corners and edges but small enough to avoid significant disturbance of the glottal airflow. A right-angle prism was placed against the glass plate, on the side opposite to the vocal fold (Fig. 1). The prism yielded two different camera views (Fig. 2), which was necessary for computation of three-dimensional physical coordinates.

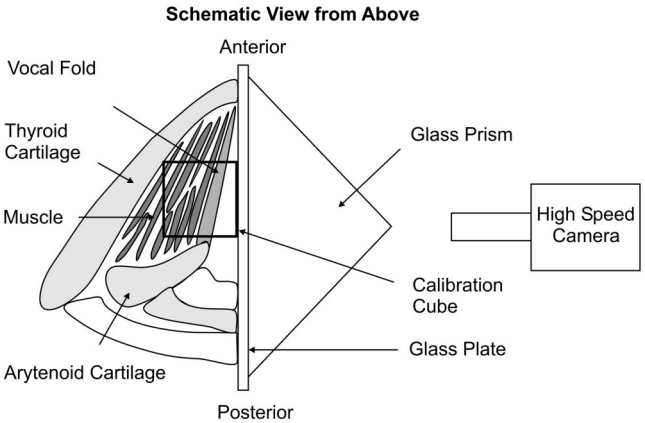

Fig. 1. Schematic experimental set-up from a superior view. On the left side of the glass plate, the hemilarynx is mounted along with a brass calibration cube. On the right side of the plate, a glass prism is mounted, providing two views of the medial surface of the vocal fold.

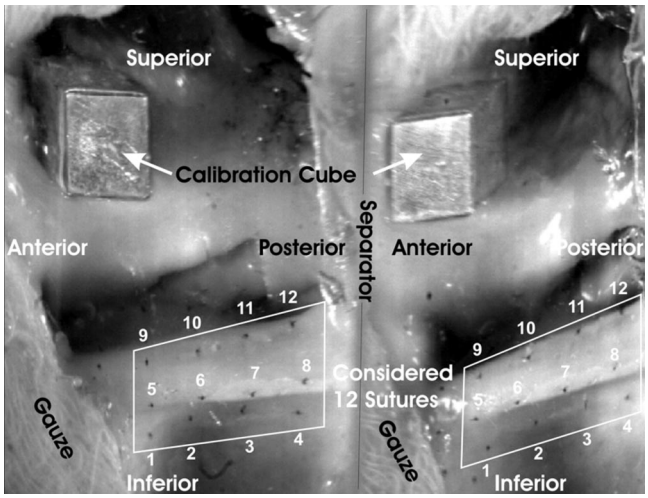

Fig. 2. A high-speed image of the medial surface of the vocal fold and the brass cube, as seen through the two faces of the prism. Altogether, 25 sutures were mounted. The 12 sutures on the medial surface that were visible within all investigated recordings are framed and numbered.

Data Acquisition

To simultaneously induce muscle contraction, muscle stiffening, medial surface bulging, and vocal fold adduction, the RLN was stimulated using a constant-current nerve stimulator (WR Medical Electronics Co. Model 2SLH, St. Paul, MN). The RLN was stimulated with a current of 0.04 to 0.08 mA at 80 Hz, with a 1.5 ms pulse duration.[3] The superior laryngeal nerve was not stimulated. The applied glottal airflow was kept nearly constant, with values ranging between 650 and 675 mL/sec (Table I).

The vibrations of the vocal fold were imaged with a high-speed digital camera (Fastcam-Ultima APX, Photron Unlimited, Inc.) using a 200 mm lens (AF MICRO NIKKOR) at a frame rate of 2,000 Hz and spatial resolution of 1,024 × 1,024 pixels. Three 150 Watt lamps served as light sources. In addition, the acoustical signal was recorded, digitized, and synchronized with the high-speed recording through means of an external trigger.

A total of eight image sequences were recorded, which included three samples of chest-like phonation (R1– R3) and five samples of fry-like phonation (R4–R8). Indeed, with unusually low fundamental frequencies (Table I) and vibrational irregularities, these latter sequences showed similarities to pulsed or fry register. Instead of a smooth vocal cycle (e.g., R3 within Fig. 3), the recordings R4 to R8 also exhibited an interruption in the movement of the vocal folds after the medial surface touched the glass plate, at the height of the lowest row of sutures. In these records, the medial surface encompassing the lower two rows of sutures stuck to the glass plate for up to two thirds of the glottal cycle (Fig. 4). Proper quantitative analyzes of the dynamics could not be computed for two recordings (R7, R8) because of vibrational irregularities (another characteristic of pulsed or fry register). The different settings (RLN stimulation and glottal flow) for the recordings are shown in Table I. The time interval for analysis for each recording was 100 ms.

Image Processing and Data Analyses

The two-dimensional position coordinates of the sutures through both prism views were computed using a semiautomatic detection program.[2] Because the upper two rows of sutures (situated superior to sutures 9–12 in Fig. 2) disappeared during a portion of the glottal cycle, it was not possible to track their movement. Also, other sutures were not extracted when their

Copyright © The American Laryngological, Rhinological and Otological Society, Inc. Unauthorized reproduction of this article is prohibited

TABLE I.
Set-up for the Eight Recordings.

	R1	R2	R3	R4	R5	R6	R7	R8
RLN (mA)	0.04	0.07	0.08	0.05	0.07	0.08	0.06	0.08
Flow (mL/s)	675	650	660	675	660	650	660	660
Ps (kPa)	1.6	2.1	1.6	2.2	3.7	3.7	3.0	2.8
TA (%)	12	33	12	37	98	98	70	61
F0 (Hz)	180	220	200	60	80	80	30	70
Sut. extracted	12	15	12	15	13	12	12	12
Quant. EEF	3	3	3	5	5	7	6	5
Sum. EEF (%)	95.9	94.7	96.9	93.7	96.1	95.0	94.3	93.9

R1 to R3 are representative of normal phonation, and R4 to R8 are reminiscent of vocal fry.
RLN = recurrent laryngeal nerve stimulation; Flow = DC airflow introduced to the trachea; Ps = measured subglottal pressure; TA= estimated percentage of maximum thyroarytenoid muscle stimulation; F_0 = computed fundamental frequency; Sut. extracted = number of sutures extracted; Quant. EEF = Number of Empirical Eigenfunctions greater than 1% considered for further computation; Sum. EEF = percentage of energy captured by the considered EEFs.

displacements were so small that they traversed only a few image pixels, yielding primarily noise. This condition occurred exclusively for the most anterior column of sutures (e.g., the column situated to the left of sutures 1, 5, 9) (Fig. 2).

Using the extracted image coordinates, the physical coordinates of the sutures were calculated using a linear approximation method.[2] Subsequently, a principal component analysis was performed to extract the Empirical Eigenfunctions (EEF) of each vibration pattern. EEFs represent a decomposition of the vibration pattern into its basic vibratory degrees of freedom.[4] In this case, the method of EEFs was used to smooth the extracted curves for further investigation. This was performed by regenerating the vibration patterns using only the most dominant EEFs (e.g., those which captured at least 1% of the vibrational energy), effectively removing higher-order noise from the trajectories. Relevant experimental settings, including the number of sutures used to compute the EEFs for each condition, are listed in Table I. All other results were shown only for the 12 sutures encircled by the white rectangle in Figure 2, which could be properly extracted across all recorded images. The following precautions were taken to report reasonable extremal values for the sutures. First, the temporal EEFs were computed to reduce high-frequency noise. Second, the vocal periods were determined within the 100 ms time interval. Next, the extremal values within each period were computed. Finally, the extremal values were averaged.

The focus of the investigation was the variation in oscillation patterns across the medial surface of the vocal fold. In par-

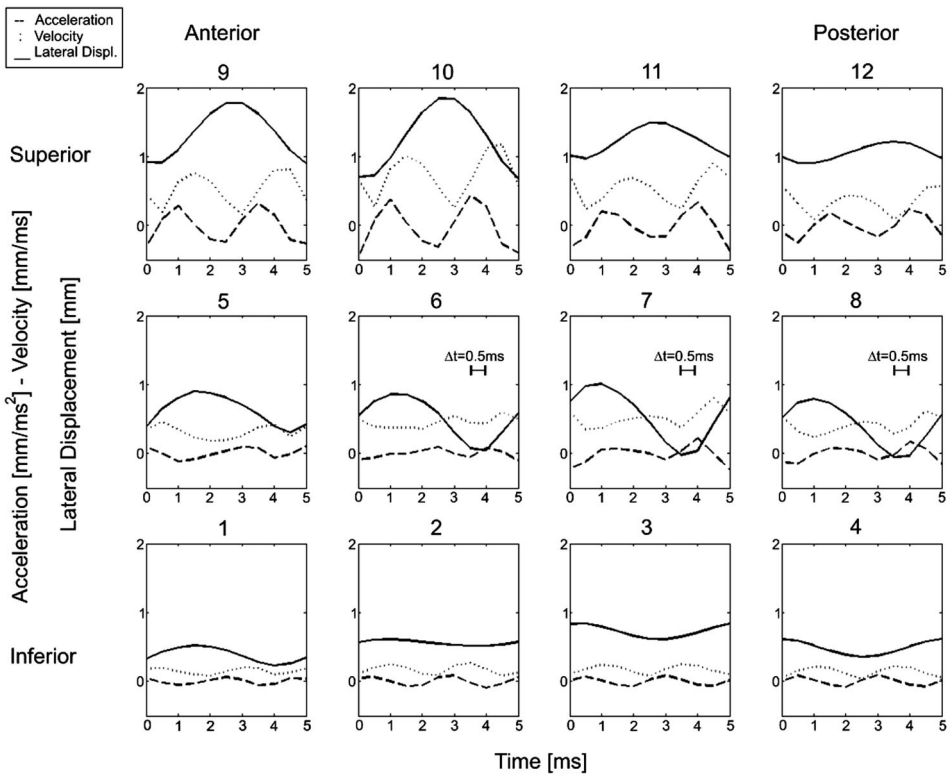

Fig. 3. Quantitative dynamical variables computed for each of the 12 sutures from recording R3, representative of normal phonation. Frames are numbered according to the suture enumeration scheme shown in Figure 2. In particular, the lateral displacement (solid lines), acceleration/deceleration (dashed), and the velocity (dotted) values are presented for one cycle. For the lateral displacement graph, zero at the vertical axis corresponds to the mounted glass plate. The bars represent glottal closure or the time interval (Δt) in which the tissue (sutures 6–8) sticks at the glass plate.

Copyright © The American Laryngological, Rhinological and Otological Society, Inc. Unauthorized reproduction of this article is prohibited

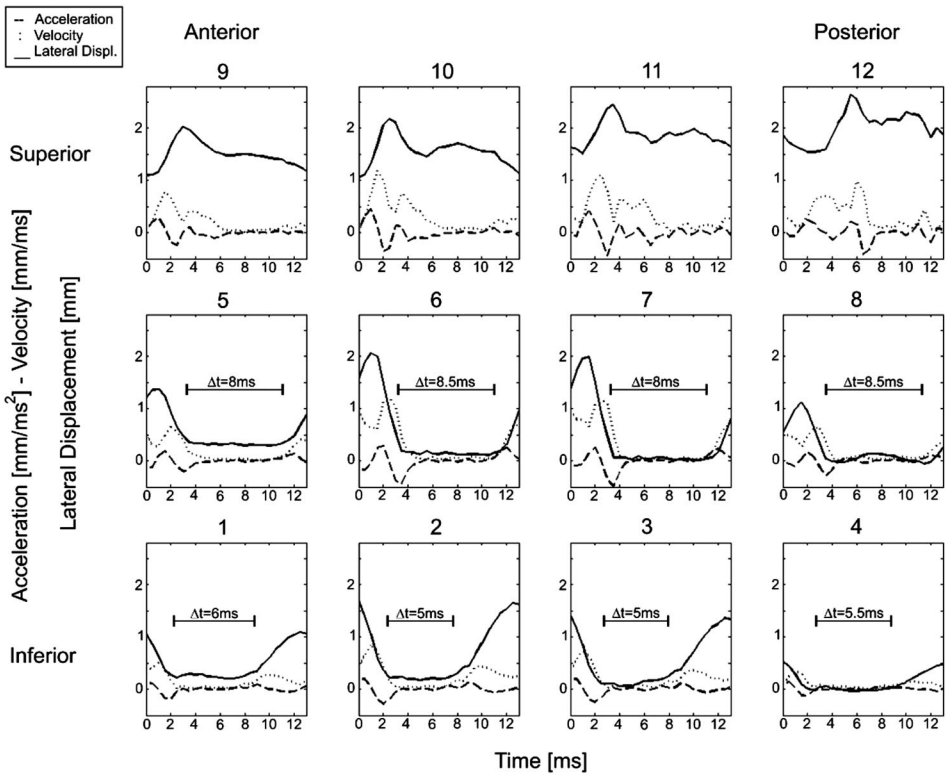

Fig. 4. Quantitative dynamical variables computed for each of the 12 sutures from recording R6, representative of fry-like phonation. Frames are numbered according to the suture enumeration scheme shown in Figure 2. In particular, the lateral displacement (solid lines), acceleration/deceleration (dashed), and the velocity (dotted) values are presented for one cycle. For the lateral displacement graph, zero at the vertical axis corresponds to the mounted glass plate. The bars represent glottal closure or the time interval (Δt) in which the tissue (sutures 1–8) sticks at the glass plate.

ticular, the study examined displacements of vocal fold fleshpoints in the lateral, vertical, and longitudinal directions as well as velocities and acceleration/deceleration values. Also, the phase delay between the different sutures was investigated. The phase delay was normalized by the period length and was computed relative to the suture in the most inferior-posterior position (no. 4, Fig. 2). Positive values indicated that the extremal values occurred later in time than the extremal values of the reference suture, and negative values indicated that they occurred before.

The glottal area function of the hemiglottis was determined by the horizontal row of sutures that yielded the minimum glottal area. Such areas were approximated using step functions.[5]

RESULTS

Experimental conditions for the different recordings are shown in Table I. The subglottal pressure varied between 1.6 to 3.7 kPa. The fundamental frequencies corresponding to normal phonation were significantly higher (180–220 Hz) than those corresponding to pathologic or fry-like phonation (30–80 Hz). Because of excessively small vibrations within R1, R3, and R5 to R8, some sutures along the most anterior column (e.g., the column situated to the left of sutures 1, 5, 9 within Fig. 2) were not taken into account for computing the EEFs. During all recordings, the upper two rows (situated superior to sutures 9–12 in Fig. 2) were not visible during portions of the glottal cycle and could not be extracted properly. These sutures were also not used for EEF computation. Therefore, depending on the phonation sample in question, 12 to 15 sutures were used to compute the EEFs (Table I). The number of separate EEFs that captured more than 1% of the entire vibrational energy was three EEFs for healthy phonation and five to seven EEFs for pathologic or fry-like phonation. For all the phonation samples, the superposition of the EEFs (which individually captured more than 1% of the vibrational energy) cumulatively captured 93.7% to 96.3% of the total energy (Table I).

To compare the different recordings, the following results were only reported for the 12 sutures, which could be extracted within all recordings. These sutures were framed and numbered from 1 to 12 within Figure 2.

For readability and overview, within Tables II, IV, VI, and VII, values of dynamical variables were differentiated based on the following background shadings: one third of the sutures with the highest values were indicated with a dark-gray background, another third with mid-range values were indicated by a light-gray background, and the remaining third with the lower values were indicated by a white background. In Tables II, IV, VI, and VII extremal values were computed as described in the previous section on image processing and data analyses. In the following discussions, the "inferior" portion of the vocal fold refers to sutures 1 to 4, the "middle" portion refers to sutures 5 to 8, and the "superior" portions refers to sutures 9 to 12. Similarly, the "anterior" portion of the vocal fold refers to sutures 1, 5, and 9; the "medial" refers to sutures 2, 3, 6, 7, 10, and 11; and the "posterior" portion refers to sutures 4, 8, and 12, (Fig. 2).

Chest-Like Phonation Samples: R1 to R3

Normal, chest-like phonation occurred for subglottal pressures ranging from 1.6 to 2.1 kPa, which corresponded to 12% to 33% of maximum thyroarytenoid muscle (TA)

Copyright © The American Laryngological, Rhinological and Otological Society, Inc. Unauthorized reproduction of this article is prohibited

TABLE II.
Averaged Maximum Values of Velocity, Acceleration, and Deceleration for Three Samples of Normal Phonation.

Sutures	R1				R2				R3			
					Velocity (mm/ms)							
9–12	0.86	1.02	1.04	0.82	1.08	1.62	1.02	0.76	1.02	1.4	1.16	0.82
5–8	0.62	0.96	1.02	0.68	0.48	0.96	1.00	0.78	0.82	0.78	1.02	0.80
1–4	0.22	0.32	0.38	0.30	0.24	0.34	0.44	0.38	0.26	0.32	0.30	0.26
					Acceleration (mm/ms^2)							
9–1	0.32	0.38	0.40	0.30	0.44	0.62	0.36	0.32	0.32	0.46	0.36	0.30
5–8	0.22	0.30	0.30	0.20	0.12	0.20	0.24	0.16	0.28	0.18	0.28	0.24
1–4	0.08	0.10	0.10	0.08	0.06	0.12	0.14	0.16	0.8	0.12	0.10	0.10
					Deceleration (mm/ms^2)							
9–12	−0.32	−0.38	−0.38	−0.28	−0.44	−0.58	−0.36	−0.30	−0.38	−0.52	−0.34	−0.28
5–8	−0.22	−0.22	−0.22	−0.14	−0.16	−0.26	−0.34	−0.26	−0.26	−0.16	−0.26	−0.20
1–4	−0.04	−0.08	−0.08	−0.08	−0.06	−0.10	−0.08	−0.12	−0.08	−0.10	−0.08	−0.10

stimulation (as estimated using Nasri et al.).[6] Velocity (mm/ms), acceleration (mm/ms^2), and deceleration (mm/ms^2) for the three samples of normal phonation are shown in Table II. Inferiorly, the extremal velocity values varied between 0.22 to 0.44 mm/ms. The anterior and posterior velocities were larger, with a maximum value of 1.08 mm/ms. The highest velocity values (dark background) were measured at the upper-medial part of the fold (0.96–1.62 mm/ms). The acceleration values were as follows: the highest values were found superiorly (up to 0.62 mm/ms^2), the medium values were located in the medial suture rows (between 0.12–030 mm/ms^2), and the lowest values were observed inferiorly (0.06–0.16 mm/ms^2). The distribution of the deceleration extrema were similar: the highest values occurred superiorly (−0.28 to −0.58 mm/ms^2), then the medially (−0.14 to −0.34 mm/ms^2), and then inferiorly (−0.04 to −0.12 mm/ms^2). The inferior decelerations were less than half the value of the medial decelerations, which in turn were smaller than the superior decelerations. For example, see the velocity (dotted) and acceleration (dashed) values for recording R3 over one cycle of vibration shown in Figure 3. The distributions of the phase delays are shown in Table III. For the velocity extrema, phase delays in the anterior-posterior direction (as referenced to suture no. 4 within Fig. 2) were relatively small. In contrast, the vertical phase delay between the inferior and medial portion of the vocal fold was between 0.20 and 0.45. The phase delay of the upper part was smaller (0.00–0.20). The phase delays of the maximum acceleration/deceleration values did not exhibit a clear structure. However, large phase delays up to 0.40 were computed for all medial and superior portions of the fold. Inferiorly, phase delays were relatively small (between -0.18 and 0.07).

In regard to vocal fold displacements, the computed maximum values are shown in Table IV. For the lateral and vertical directions, the smallest amplitudes of vibration occurred inferiorly (lateral 0.11–0.62 mm, vertical 0.22–0.49 mm). In the anterior-posterior direction, the smallest values occurred posteriorly (0.07–0.11 mm). As denoted by the shadings within Table IV (dark gray: high values, white: low values), the highest values for the lateral displacements occurred medially and superiorly. For the vertical and longitudinal displacements, the maximum values occurred superiorly. In regard to the lateral displacements, extrema situated in the superior and middle rows were usually more than double the value of the extrema located in the inferior row. For the vertical displacements, the amplitudes in the superior row were approximately two times larger than the amplitudes in the middle row and approximately 3 times larger than the

TABLE III.
Phase Delays for Velocity, Acceleration/Deceleration Relative to suture 4 (the Most Inferior-Posterior Suture) for the Three Samples of Regular Phonation.

Sutures	R1				R2				R3			
	Phase delay of velocity extremal values											
9–12	0	0	0.16	0.16	0.11	0.11	0.14	0.17	0.13	0.13	0.18	0.20
5–8	0.30	0.25	0.23	0.25	0.31	0.31	0.28	0.28	0.45	0.33	0.20	0.23
1–4	0.07	0.11	0.02	0	0	0	0.03	0	−0.13	−0.03	0	0
	Phase delay of acceleration/deceleration extremal values											
9–12	0.25	0.27	0.14	0.16	0.08	0.14	0.19	0.25	0.35	0.10	0.13	0.20
5–8	0.25	0.25	0.23	0.23	0.31	0.31	0.28	0.28	0.40	0.25	0.18	0.20
1–4	0.07	0.07	0	0	0	0	0.03	0	−0.18	−0.05	0	0

Copyright © The American Laryngological, Rhinological and Otological Society, Inc. Unauthorized reproduction of this article is prohibited

TABLE IV.
Averaged Maximum Values for Displacement Amplitudes for the Sutures from the Three Samples of Normal Phonation.

Sutures	R1				R2				R3			
	Lateral (mm)											
9–12	1.23	1.57	1.05	0.74	1.11	1.47	0.69	0.39	1.03	1.35	0.61	0.35
5–8	0.92	1.32	1.39	0.92	0.55	1.07	1.21	0.98	0.75	0.94	1.18	0.97
1–4	0.20	0.32	0.62	0.49	0.25	0.37	0.55	0.51	0.32	0.11	0.27	0.29
	Vertical (mm)											
9–12	0.88	1.24	1.30	0.89	0.95	1.36	1.20	0.80	1.08	1.59	1.35	0.90
5–8	0.29	0.52	0.58	0.46	0.26	0.54	0.55	0.37	0.49	0.72	0.71	0.46
1–4	0.24	0.41	0.38	0.25	0.28	0.37	0.49	0.22	0.22	0.46	0.40	0.30
	Longitudinal (mm)											
9–12	0.28	0.27	0.25	0.07	0.31	0.32	0.22	0.07	0.34	0.32	0.19	0.08
5–8	0.17	0.16	0.14	0.09	0.08	0.19	0.13	0.07	0.24	0.17	0.17	0.11
1–4	0.07	0.11	0.11	0.08	0.08	0.11	0.13	0.07	0.09	0.12	0.14	0.10

amplitudes in the inferior row. Overall, the displacement, velocity, acceleration, and deceleration values were greater in the middle part of the vocal fold than in the anterior and posterior parts (Tables II and IV). For example, the computed lateral displacements (solid lines) of the sutures for recording R3 over one glottal cycle are shown in Figure 3.

The displacement phase delay distribution is shown in Table V. Again, the horizontal phase delays were negligible. The largest phase delays (relative to suture no. 4) occurred at the superior suture row (lateral 0.28–0.65, vertical 0.08–0.27, longitudinal 0.03–0.23). The next largest phase delays occurred at the middle suture row (lateral 0.08–0.35, vertical 0.00–0.09, longitudinal —0.06–0.18).

Fry-Like Phonation Samples: R4 to R6

Fry-like phonation occurred for subglottal pressures ranging from 2.2 to 3.7 kPa, which corresponded to 37% to 98% of maximum TA stimulation (as estimated using Nasri et al).[6] As mentioned earlier, the vibrations within recordings R7 and R8 were highly aperiodic, and no displacement-velocity analyzes could be performed. Therefore, the results for pathological or fry-like phonation were restricted to recordings R4 to R6. In addition, for R4 to R6, no phase delay tables were shown. This is because no observable structure within the recordings could be identified, perhaps because the tissue stuck against the glass plate for up to 65% of the total vibration cycle (see sutures 1–8 of recording R6 in Fig. 4), obscuring the identification of extremal values.

In Table VI, the computed maximum values for the displacements are shown. Although, there is no clear structure as within the normal phonation values (Table IV), the grayscale encoding (dark-gray: high values, white: low values) suggests maximal displacement in the superior-medial portion of the vocal fold. The smallest displacements appeared to occur inferiorly. The largest third of the lateral displacements varied between 1.22 mm and 2.33 mm, and the smallest third was calculated at 0.58 mm to 1.19 mm. In the vertical direction, the largest third varied from 0.87 mm to 2.05 mm, and the smallest

TABLE V.
Phase Delays for Displacement Relative to Suture 4 (the Most Inferior-Posterior Suture) from the Three Recorded Samples of Normal Phonation.

Sutures	R1				R2				R3			
	Phase delay of lateral extremal values											
9–12	0.45	0.45	0.59	0.59	0.28	0.28	0.31	0.33	0.55	0.50	0.55	0.65
5–8	0.23	0.18	0.18	0.18	0.17	0.14	0.08	0.14	0.35	0.25	0.20	0.20
1–4	0.18	0.05	0	0	0.08	0.06	0	0	0.30	0.20	0.10	0
	Phase delay of vertical extremal values											
9–12	0.14	0.18	0.23	0.27	0.08	0.08	0.11	0.17	0.10	0.10	0.15	0.20
5–8	0.05	0.05	0.05	0.09	0.03	0.03	0.03	0.03	0.05	0	0	0
1–4	0	0	0	0	0	−0.03	−0.03	0	0	−0.05	0	0
	Phase delay of longitudinal extremal values											
9–12	0.14	0.18	0.27	0.23	0.03	0.09	0.011	0.14	0.10	0.10	0.05	0.20
5–8	−0.05	0	0.05	0.18	−0.06	−0.06	−0.03	−0.03	−0.05	−0.05	0	0.05
1–4	−0.14	−0.14	−0.05	0	−0.09	−0.09	−0.06	0	−0.20	−0.15	−0.10	0

Copyright © The American Laryngological, Rhinological and Otological Society, Inc. Unauthorized reproduction of this article is prohibited

TABLE VI.
Averaged Maximum Values for Displacement Amplitudes for the Sutures from the Samples of Fry-Like Phonation.

Sutures	R4				R5				R6			
					Lateral (mm)							
9–12	0.67	1.09	0.86	0.58	1.64	2.07	1.10	0.76	1.19	1.48	1.22	1.52
5–8	0.91	1.30	1.31	0.86	1.17	2.17	2.14	1.16	1.29	2.32	2.33	1.29
1–4	0.83	1.26	1.22	0.69	0.90	1.78	1.62	0.88	1.06	1.65	1.45	0.67
					Vertical (mm)							
9–12	0.66	1.03	1.13	0.83	1.35	1.99	1.90	1.42	1.12	2.03	2.05	1.50
5–8	0.35	0.69	0.78	0.52	0.69	1.29	1.45	0.59	0.55	1.29	1.38	0.55
1–4	0.44	0.80	0.87	0.57	0.36	0.70	0.67	0.28	0.24	0.61	0.44	0.09
					Longitudinal (mm)							
9–12	0.26	0.27	0.20	0.08	1.08	0.77	0.32	0.29	0.48	0.46	0.62	0.41
5–8	0.24	0.18	0.16	0.05	0.48	0.78	0.18	0.06	0.37	0.46	0.36	0.17
1–4	0.12	0.14	0.14	0.14	0.16	0.53	0.14	0.09	0.09	0.24	0.15	0.17

third from 0.09 mm to 0.67 mm. In the anterior-posterior direction, the highest values varied from 0.20 mm to 1.08 mm and the smallest values from 0.05 mm to 0.29 mm. For example, the computed lateral displacements (solid lines) of the sutures for recording R6 over one glottal cycle are shown in Figure 4. As noted previously, the sutures 1 to 8 stuck to the glass plate (0 at the vertical axis, resulting in glottal closure) for up to 65% (Δt) of the glottal cycle.

Within the velocity/acceleration-deceleration distribution (Table VII), a clearer picture can be seen. The highest velocities were found in the superior-medial region of the fold (0.94–1.76 mm/ms). The smallest velocity values (0.30–0.58 mm/ms) were computed in the inferior-anterior and inferior-posterior regions. The distribution of the acceleration and deceleration values were similar. The highest values occurred in the superior-medial region (accelerations up to 0.60 mm/ms^2 and decelerations up to -0.76 mm/ms^2 at R6). The lowest values were again computed in the inferior-anterior (-0.06 mm/ms^2 at R4) and inferior-posterior regions (-0.08 mm/ms^2 at R4). For example, the computed velocity (dotted) and acceleration/deceleration (dashed) values for recording R6 over one glottal cycle are shown in Figure 4. Although sutures 1 to 8 stick to the glass plate over a large portion of the glottal cycle, it is clear that their values remain constant during this time interval.

Computed Hemiglottis Area: R1 to R6

The hemiglottis areas for R1 to R6 over one glottal cycle are shown in Figure 5. The initiation of these plots corresponds to the time when suture number 4 begins moving toward the glass plate. For the normal vibration patterns (R1–R3), the following behavior was observed: after a slight increase in the glottal area, the area decreased until it increased more steeply in the last third of the vibration cycle. For each of the three recordings, the computed glottis time closure (<1 mm^2) was approximately 0.5 ms. This was between 9% and 11% of the total glottal cycle.

For the pathologic or fry-like vibrations (R4–R6), the sticking of the tissue to the glass plate yielded a relatively long glottal closure in the middle of each cycle. The com-

TABLE VII.
Averaged Maximum Values for Velocity, Acceleration, and Deceleration from the Samples of Fry-Like Phonation.

Sutures	R4				R5				R6			
					Velocity (mm/ms)							
9–12	0.76	1.26	0.96	0.66	1.32	1.58	1.10	1.00	1.00	1.58	1.46	1.42
5–8	0.64	0.94	1.00	0.80	0.72	1.42	1.42	0.90	0.82	1.76	1.74	0.80
1–4	0.30	0.52	0.54	0.36	0.50	1.16	1.02	0.50	0.58	1.06	0.92	0.48
					Acceleration (mm/ms^2)							
9–12	0.30	0.52	0.44	0.26	0.46	0.50	0.40	0.28	0.38	0.60	0.56	0.56
5–8	0.12	0.18	0.18	0.28	0.18	0.28	0.22	0.22	0.26	0.48	0.42	0.22
1–4	0.06	0.12	0.16	0.12	0.14	0.32	0.24	0.16	0.16	0.28	0.26	0.18
					Deceleration (mm/ms^2)							
9–12	−0.28	−0.56	−0.42	−0.28	−0.36	−0.48	−0.44	−0.42	−0.36	−0.54	−0.56	−0.38
5–8	−0.26	−0.44	−0.26	−0.36	−0.28	−0.52	−0.44	−0.36	−0.34	−0.76	−0.74	−0.28
1–4	−0.06	−0.12	−0.10	−0.08	−0.18	−0.34	−0.30	−0.18	−0.26	−0.48	−0.42	−0.16

Copyright © The American Laryngological, Rhinological and Otological Society, Inc. Unauthorized reproduction of this article is prohibited

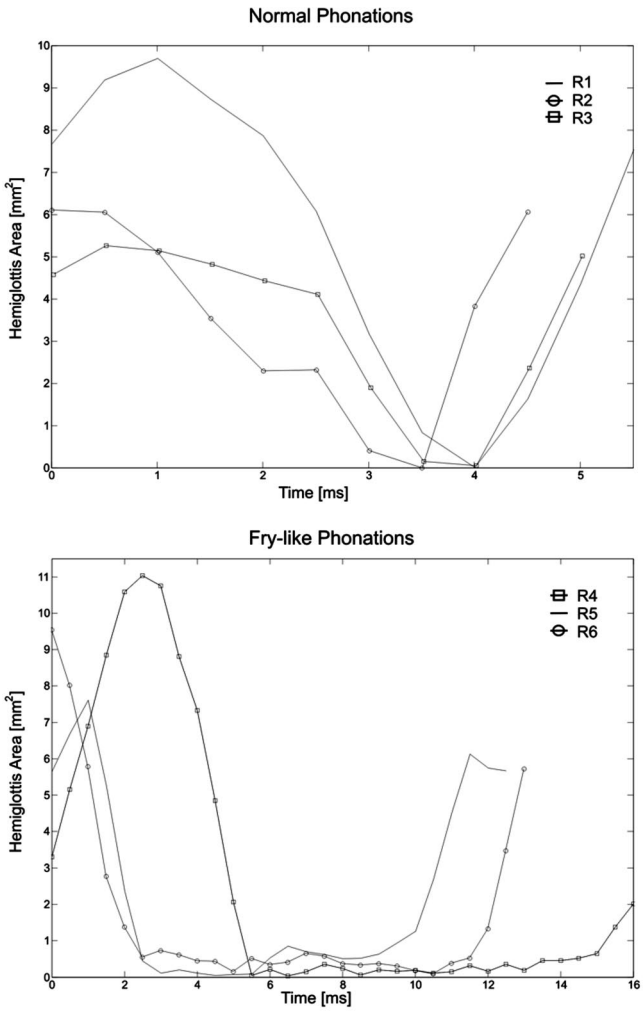

Fig. 5. Hemiglottis areas for samples of normal phonation (upper chart) and fry-like phonation (lower chart). For fry-like phonation, the sticking of the tissue to the glass plate (glottal closure) is represented by the prolonged, low-level hemiglottis area (<1 mm^2).

puted glottal closure (<1 mm^2) intervals were as follows, expressed as percentages of the glottal cycle: 59% (R4), 64% (R5), and 69% (R6). The maximum glottal areas (7.5–11.2 mm^2) were slightly higher but still in the same range as those for normal phonation (5.3–9.8 mm^2).

DISCUSSION

This study reported quantitative measurements of the medial surface dynamics of an in vivo canine vocal fold using a hemilarynx methodology and high-speed digital imaging. Traditionally, quantitative investigations have been performed using endoscopic techniques, which image only a superior view of the folds,[7] neglecting many aspects of mucosal wave propagation. On the other hand, direct measurement of the medial surface dynamics of the folds have helped to increase our knowledge of mucosal wave propagation, a critical component of vocal fold vibration.[8,9] Moreover, in vivo models allow us to observe vibrations under realistic conditions in which simultaneous muscle contraction, muscle stiffening, medial surface bulging, and vocal fold adduction occur.[3]

In regard to the experimental set-up of the in vivo canine, the visibility of the superiorly mounted sutures needs to be improved. This limitation has already been surmounted for the excised human larynx, but canine laryngeal anatomy presents additional challenges. Possible solutions could include the use of a second camera or the use of mirrors to increase the field of vision.

The original design of this experiment was to report a variety of vibrations as a function of the stimulation current to the RLN. However, stimulation current was not a stable input measure with which to differentiate the different vibrations patterns. As shown in earlier work,[6] the TA stimulation (as measured by electromyography [EMG]) is a sigmoidal function of the RLN stimulation current (or voltage). In particular, over a very narrow range of RLN stimulation current, the TA activity varied from 0% to 100% of maximum stimulation. Thus, with only a small amount of input noise, the resultant TA activity may be completely unknown. Perhaps because of this phenomenon, in the present study, the recorded vibration patterns occurred randomly with respect to the input RLN stimulation current.

Nevertheless, the Nasri et al.[6] study also reported that robust measures of TA activity (expressed in percentage of maximum stimulation) could be estimated on the basis of the dynamical range of input pressure (see Fig. 5 in Nasri et al).[6] For the present study, the dynamical range of subglottal pressures was 1.2 to 3.7 kPa. Using this empirical relationship from Nasri et al.,[6] we could see periodic, chest-like phonation in the range of 12% to 33% of maximum TA stimulation. Fry-like phonation was observed in the range of 37% to 98% of maximum TA stimulation, characterized by low fundamental frequencies (30–80 Hz), irregular oscillations, and pulse-like vibrations, with relatively long periods of glottal closure. Within the range of chest-like vibrations, fundamental frequency increased with increasing TA activity. However, beyond a certain threshold of TA activity, fundamental frequency abruptly dropped, resulting in fry-like vibrations, as already discussed. Similar phenomena have been observed and predicted previously.[10–13] For example, it is known that TA activity causes the TA muscle to simultaneously stiffen and contract. If the muscle itself were a significant component of the vibrating tissue (presumably this would be the case in chest voice), as TA activity were increased, the increased stiffness of the TA would result in an increase in the fundamental frequency. However, if the tissue vibrations only occurred in the cover (presumably this would be the case in vocal fry), as TA activity were increased, the contraction of the TA would also shorten the cover, decreasing the stiffness in the cover, and thereby decreasing the fundamental frequency. In future studies, it will be important to measure the complex potential directly at the TA or at other branches of the RLN with EMG.

As in previous studies,[9,14] only a few EEFs were necessary to capture the essential dynamics of the vocal fold ($>93.5\%$). For the normal phonation samples, only three significant EEFs were excited (e.g., only 3 EEFs captured more than 1% of the energy). For the fry-like phonation samples that exhibited low frequencies, long

Copyright © The American Laryngological, Rhinological and Otological Society, Inc. Unauthorized reproduction of this article is prohibited

closure times, and frequent aperiodicities, five to seven EEFs were excited (e.g., 5–7 EEFs captured more than 1% of the energy) to capture the increased complexity of the system.

In regards to the velocity/acceleration results (Tables II and VII), these were comparable with earlier experimental measurements using excised larynges.[8,15] The results clearly suggest an inhomogeneous spatial distribution of the measured dynamical variables (e.g., the dynamical variables across the different sutures varied considerably). The phase delays (Tables III and V) between the different parts of the vocal fold reflected the dynamics of a traveling wave, yielding data to evaluate parametric models of mucosal wave propagation.[15–17] The lack of an obvious phase delay within the pathologic recordings further suggested the importance of the mucosal wave in normal voice production.[1]

Across samples of both normal and fry-like phonation, vocal fold displacements (Tables IV and VI) showed similar amplitudes of vibration in both the lateral and vertical directions. This suggests that endoscopic measurements of vocal fold vibration ignore a major component of the laryngeal dynamics (i.e., vertical displacements). This also suggests a potentially critical limitation of many well-known mathematical models of vocal fold vibration that neglect vertical displacements. Also, in the fry-like phonation samples (Table VI), the anterior-posterior displacements were relatively large compared with such displacement in normal phonation (Table IV). Although the reason for this latter observation is not known, it may be that anterior-posterior vibrations cannot be neglected in certain types of irregular phonation. For both normal and fry-like phonation, the measured dynamical variables (displacements, velocities, etc.) showed a correspondence with fundamental frequency (Table I). That is, the higher the fundamental frequency, the larger the amplitudes of the dynamical variables. Also, the extracted glottal areas for the normal phonation (Fig. 5) were similar to glottal areas reported previously.

CONCLUSIONS

Detailed quantitative measurements were reported regarding the medial surface dynamics of an in vivo canine vocal fold. Such measurements are unique, shedding light on many previously unstudied aspects of mucosal wave propagation, including physiologic and dynamic differences between chest-like and fry-like vibration patterns. Such measurements are critical to evaluate and refine computational models of vocal fold vibration. Future investigations of both RLN and superior laryngeal nerve stimulation and their influence on vocal fold dynamics are in progress.

BIBLIOGRAPHY

1. Schoenhaerl E. *Die Stroboskopiein der Praktischen Laryngologie*. Stuttgart: Thieme-Verlag, 1960.
2. Doellinger M, Berke GS, Berry DA. Medial surface dynamics of an in vivo canine vocal fold during phonation. *J Acoust. Soc. Am* 2005;117:3174–3183.
3. Bielamowicz S, Berke GS, Kreiman J, Gerratt BR. Exit jet particle velocity in the in Vivo canine laryngeal model with variable nerve stimulation. *J Voice* 1999;13:153–160.
4. Berry DA, Montequin DW, Tayama N. High-speed digital imaging of the medial surface of the vocal folds. *J Acoust Soc Am* 2001;110:2539–2545.
5. Bronstein IN, Semendjajew KA. *Taschenbuch der Mathematik.* Stuttgart: Verlag Harry Deutsch, 1979.
6. Nasri S, Dulguerov P, Damrose EJ, et al. Relation of recurrent laryngeal nerve compound action potential to laryngeal biomechanics. *Laryngoscope* 1995;105:639–643.
7. Schuberth S, Hoppe U, Doellinger M, et al. High-precision measurement of the vocal fold length and vibratory amplitudes. *Laryngoscope* 2002;112:1043–1049.
8. Baer T. *Investigation of Phonation Using Excised Larynges.* Boston: Massachusetts Institute of Technology, PhD Thesis, 1975.
9. Berry DA. Mechanisms of modal and non-modal phonation. *J Phonet* 2001;29:41–50.
10. Hirano M. Morphological structure of the vocal cord as a vibrator and its variations. *Folia Phoniatrica* 1974;26: 89–94.
11. Hirano M. Phonosurgery: basic and clinical investigations. *Otologia (Fukuoka)* 1975;21:239–440.
12. Titze IR, Jiang JJ, Druker D. Preliminaries to the body-cover theory of pitch control. *J Voice* 1988;1:314–319.
13. Titze IR. *Principles of Voice Production*. Englewood Cliffs, NJ: Prentice-Hall, 1994.
14. Alipour F, Berry DA, Titze IR. A finite element model of vocal fold vibration. *J Acoust Soc Am* 2000;108:3003–3012.
15. Titze IR, Jiang JJ. A measurement of mucosal wave propagation and vertical phase difference in vocal fold vibration. *Ann Otol Rhinol Laryngol* 1993;102:58–63.
16. Jiang JJ, Chang CI, Raviv JR, et al. Quantitative study of mucosal wave via videokymography in canine larynges. *Laryngoscope* 2000;110:1567–1573.
17. Berry DA, Clark MJ, Montequin DW, Titze IR. Characterization of the medial surface of the vocal folds. *Ann Otol Rhinol Laryngol* 2001;110:470–477.

Copyright © The American Laryngological, Rhinological and Otological Society, Inc. Unauthorized reproduction of this article is prohibited